XLI CILAMCE
XLI Ibero-Latin American Congress on Computational Methods in Engineering
16-19 November, 2020 FOZ DO IGUAÇU PARANÁ - BRAZIL

Probabilistic analysis of the corrosion initiation in concrete structures subjected to chloride ingress using the Boundary Element Method

Vinícius de B. Souza[1], Edson D. Leonel[1]

[1]*Dept. of Structural Engineering, São Carlos School of Engineering, University of São Paulo*
Av. Trabalhador São Carlense, 400, 13566-590, São Carlos, São Paulo, Brazil
viniciuswg@hotmail.com; edleonel@sc.usp.br

Abstract. Reinforcement's corrosion is the main cause of durability reduction in reinforced concrete structures. Besides, the chloride ingress is the main agent in this problem. The reinforcement's corrosion process occurs in two stages: in the first, known as the initiation period, chloride ions penetrate into concrete pores and accumulate at the concrete/reinforcement interface, which lead to the depassivation when the threshold concentration is reached. After the depassivation, the propagation period starts, which triggers the reinforcement's corrosion and the structural collapse. Because of the faster structural safety reduction observed in the latter stage, the initiation period is often adopted as structural service life. In this regard, this study applies the two-dimensional transient formulation of the Boundary Element Method (BEM) for the chloride diffusion modelling. Because of the non-requirement of the domain mesh, the chloride concentrations at the domain are accurately assessed. Moreover, this problem is properly analysed solely in the probabilistic context because of the huge randomness over the governing variables. The Monte Carlo Simulation assesses the probabilities of failure herein, which accounts for the failure scenarios described by the BEM. In addition to the phenomenological random variables, cracks positioned at the cover account for the inherent concrete cracking and describe preferential ingress paths.

Keywords: Boundary Element Method, Probabilistic Modelling, Chloride Penetration.

1 Introduction

The concern with structural durability is intrinsically related to the safety of the structure and its users. In addition to the safety aspects, another factor reinforces this concern: the economic. In developed or developing countries, the monetary losses due to the rehabilitation of structures deteriorated by corrosion revolve around 1.25% to 3.5% of the country's GDP (Gross Domestic Product) [1]. In the case of reinforced concrete (RC) structures, corrosion may significantly influence the long-term performance, especially in aggressive environments. Chlorides ions, in particular, increase the electrical conductivity of the electrolyte, accelerating the corrosion process and destroying the passive film on the reinforcement (called depassivation of steel reinforcement), causing pitting corrosion, which presents a high risk for RC structures [2]. Diffusion is one of the main mechanisms for transporting chloride ions through concrete [3,4], being diffusion models predominating in the literature. It is also recognized that cracks provide easy access to ingress of chlorides in concrete and affect its durability properties with most significant effect on the depassivation of reinforcements, reducing the corrosion initiation time [5,6]. According to Zhang et al. [7], disregarding concrete cracking can lead to an overestimation of the service life of a structure.

There are several methodologies for evaluating the initiation period. However, many of them present huge restrictions and strong simplifications in their modelling assumptions. These comments are particularly valid for analytical approaches, which stimulated the development of numerical schemes. The Boundary Element Method (BEM) is a numerical method capable of representing accurately the chloride diffusion into concrete pores. Despite this approach has not been widely used for this purpose, the BEM has considerable advantages over other numerical approaches, such as discretization applied solely at the geometry boundary and reduction in one dimension of the mesh in relation to the dimension of the problem, which reduces the number of degrees of

freedom and the system of equations. For its considerable advantages, this study applies the transient BEM formulation for analysing the corrosion initiation triggered by chloride diffusion into two-dimensional cracked structures. The subregion BEM technique enables the representation of dissimilar materials and cracks. Besides, the uncertainties of the phenomenon of diffusion are quantified herein through the Monte Carlo Simulation technique. One application demonstrates the robustness of the proposed approach, which may suggest fair values for cover depth as a function of the probability of failure.

2 The Transient Boundary Element Method

2.1 Integral equation for potential problems

The transient potential problem utilises the following diffusion equation:

$$\nabla^2 u - \frac{1}{k}\frac{\partial u}{\partial t} = 0, \tag{1}$$

where *u* is potential, *t* is time and *k* is the diffusion coefficient. According to Wrobel [8], the problem definition is completed with the specification of boundary conditions in potential (u) and flux (q), respectively:

$$\begin{aligned} u(x,t) &= \overline{u}(x,t)\; x \in T_1\;, \\ q(x,t) &= \overline{q}(x,t)\; x \in T_2\;, \end{aligned} \tag{2}$$

and initial conditions:

$$u(x,t) = \overline{u}(x,t_0)\; x \in \Omega\;, \tag{3}$$

in which $\overline{u}$ is the prescribed potential value, $\overline{q}$ indicates the prescribed flux value, x is the field points, t_0 the initial time, $\Gamma = \Gamma_1 \cup \Gamma_2$ represents the boundary and Ω the problem domain.

Equation (1) leads to a boundary integral representation by applying the Time-Dependent Fundamental Solution available in Wrobel [8]. Assuming as nil the initial condition in the domain, this approach provides the following equation, in which temporal and spatial integration are required [8]:

$$c(\xi)\,u(\xi,t_F) + k\int_{t_0}^{t_F}\int_{\Gamma} u(x,t)\,q^*(\xi,x,t_F,t)\,d\Gamma\,dt = k\int_{t_0}^{t_F}\int_{\Gamma} q(x,t)\,u^*(\xi,x,t_F,t)\,d\Gamma\,dt, \tag{4}$$

where ξ indicates the source points (points where the potential or flux is applied), t_F the observation time, u^* and q^* are the time-dependent fundamental solutions for potential and flux, respectively, and c is the BEM free term. In the cases where the source point is positioned at smooth boundary geometries, the value of c equals 0.5. For two-dimensional problems, the time-dependent fundamental solutions are as follows:

$$u^*(\xi,x,t_F,t) = \frac{1}{4\pi k\tau}\exp\left(-\frac{r^2}{4k\tau}\right), \tag{5}$$

$$q^*(\xi,x,t_F,t) = -\frac{r}{8\pi k^2\tau^2}\frac{\partial r}{\partial \eta}\exp\left(-\frac{r^2}{4k\tau}\right), \tag{6}$$

in which $\tau = t_F - t$, and r indicates the distance between the source point and the field point.

2.2 Numerical solution

The Equation (4) can be rewritten by inverting the order of integration and dividing the boundary of the problem into *Ne* boundary elements and the time $t_F - t_0$ into *NT* time steps. Thus:

$$c_i u_i^{NT} = k\sum_{j=1}^{Ne}\sum_{n=1}^{NT}\int_{\Gamma_j}\int_{t_0^n}^{t_F^n} q^n u^* dt\, d\Gamma \;\; - k\sum_{j=1}^{Ne}\sum_{n=1}^{NT}\int_{\Gamma_j}\int_{t_0^n}^{t_F^n} u^n q^* dt\, d\Gamma\,, \tag{7}$$

where u_i^{NT} is the value of the potential in the source point *i* at time $t = NT$, t_0^n and t_F^n are, respectively, the initial and last time in the step time *n*. Assuming that source points have been positioned at smooth boundaries and the values of u^n and q^n are constant in each time step, the previous equation can be rewritten as follows:

$$\sum_{n=1}^{NT}\sum_{j=1}^{Ne} H_{ij}^n u_j^n = \sum_{n=1}^{NT}\sum_{j=1}^{Ne} G_{ij}^n q_j^n\,, \tag{8}$$

where:

$$H_{ij}^n = \begin{cases} k\int_{\Gamma_j}\int_{t_0^n}^{t_F^n} q^* dt\, d\Gamma + 0{,}5 \quad if \;\; n = 1 \;\; and \;\; i = j, \\ \qquad k\int_{\Gamma_j}\int_{t_0^n}^{t_F^n} q^* dt\, d\Gamma \quad otherwise. \end{cases} \tag{9}$$

$$G_{ij}^n = k\int_{\Gamma_j}\int_{t_0^n}^{t_F^n} u^* dt\, d\Gamma\,. \tag{10}$$

The system of algebraic equations is obtained by applying Equation (8) for every boundary node. This system can be written in terms of classical BEM matrices *G* and *H*, which contains, respectively, the kernels u^* and q^* [9]:

$$\sum_{n=1}^{NT}\Big[G^{NT+1-n}\Big]\{q^n\} = \sum_{n=1}^{NT}\Big[H^{NT+1-n}\Big]\{u^n\}, \tag{11}$$

where $\{q\}$ and $\{u\}$ are vectors of flux and potential, respectively at the boundary. The solution of Equation (11) requires the classical columns change procedure, which enables the vector of known $\{f^{NT}\}$ and unknown $\{x^{NT}\}$ quantities at the boundary at each time step. This procedure leads to the columns change between matrices *G* and *H* of the first time step, providing matrices A and B, which are used in the solution of the entire problem, according to Equation (12) [9].

$$\Big[A\Big]\{x^{NT}\} = \Big[B\Big]\{f^{NT}\} + \sum_{n=1}^{NT-1}\Big[G^{NT+1-n}\Big]\{q^n\} - \Big[H^{NT+1-n}\Big]\{u^n\}\;. \tag{12}$$

The singular kernels in Equation (9) and (10) have been regularized by the Singularity Subtraction Technique whereas the non-singular kernels have been integrated by the Gauss-Legendre quadrature.

3 The subregion technique

The above BEM formulation is valid only for homogeneous domains. This limitation can be avoided by introducing the subregion technique, which allows for incorporating materials with different diffusion coefficient. The technique was proposed by Rizzo & Shippy [10] and consists of discretising the nonhomogeneous domain into homogeneous regions, known as subregions, where the continuity between them is enforced by applying the compatibility of potential and equilibrium of fluxes. Thus:

$$u_i^S = u_i^Z\,, \tag{13}$$

$$q_i^S = -q_i^Z\,, \tag{14}$$

in which i indicates the node positioned at the interface of adjacent subregions S and Z, with $S \neq Z$.

Considering a problem defined over a domain which is only piecewise homogeneous, the Eq. (9) and Eq. (10) are applied to each subregion independently. Then, matrices *G* and *H* of each subregion, obtained independently, are strategic allocated in order to provide global matrices for the entire domain. Also vectors $\{u\}$ and $\{q\}$ are manipulated to store the quantities at the boundary of each subregion. Nevertheless, this system of equations is undetermined because both potential and flux are unknown for each node positioned at the interfaces. By introducing Eq. (13) and Eq. (14), the final system of equations becomes determined and the domain continuity is re-established. Then, the numerical procedure for solving the final system can be performed through Eq. (12).

The subregion technique can also be applied to represent co-planar crack surfaces in homogeneous or nonhomogeneous bodies. In this approach, artificial boundaries are introduced in the domain for dividing the cracked body into subregions, where each subregion containing one crack surface [11]. Then, Eq. (13) and Eq. (14) represent the closed crack faces conditions and the crack surfaces are external boundaries. It is worth stressing that the crack width is not required and any additional equation is not introduced to this approach.

4 The Monte Carlo Simulation

The Monte Carlo Simulation (MCS) is a numerical simulation technique developed by Metropolis & Ulam [12], which uses sequences of random numbers with uniform distribution between 0 and 1 for indicating the Probability Density Function $f_X(x)$ value of each random variable. In structural engineering applications, the MCS usually assesses the probability of failure (P_f) of complex structures and structural systems subject to randomness. The failure scenarios are evaluated through the limit state equation, in which an indicator function $I[x]$ assigns a unitary value if x belongs to the failure domain or zero, otherwise. By definition:

$$P_f = \int_{\Omega} I[x] f_X(x)\, dx. \tag{15}$$

The above equation can be estimated using a finite number of samples (n_S), according to:

$$P_f \approx \hat{P}_f = \frac{1}{n_S} \sum_{j=1}^{n_S} I[x_j] = \frac{n_f}{n_S}, \tag{16}$$

in which n_f is the number of samples in the failure domain and $\hat{P}_f$ is the estimated probability of failure. Thus, the direct result of MCS is the probability of failure. However, it is possible to obtain an equivalent reliability index (β) through the distribution function of standardized normal distribution (Φ):

$$\beta = -\Phi^{-1}(\hat{P}_f). \tag{17}$$

The MCS is widely associated with BEM, since the BEM has recognized computational efficiency and accuracy in several engineering problems. In this study, the BEM provides the concentration of chloride $C(x,t)$ at concrete cover depth x and time t. From a known chloride threshold content value (C_r), the MCS accesses the probability of failure by the following limit state equation (G):

$$G(x,t) = C_r - C(x,t). \tag{18}$$

The chloride threshold has been often represented by a deterministic value, which is obtained accounting for the class of environmental aggressiveness and concrete composition. Nevertheless, this quantity has important randomness behaviour, which suggests that C_r should be randomly modelled instead of deterministically.

5 Numerical example

This application presents the corrosion time initiation analysis of a typical cross-section from a reinforced concrete beam. One assumes the structure as positioned along the coastal zone, being exposed to chloride ions (Cl^-) on its side and bottom boundaries. The upper boundary has been covered by a resin, which prevents the chloride ingress

from that position. Then, flux is nil along the upper boundary, as illustrated in the fig. 1a. The cross-section dimensions are 300 mm x 480 mm and it has been reinforced with eight rebars of diameter $\phi = 25$ mm (fig. 1b). Shaikh [6], suggests the formation of cracks are unavoidable along the concrete because of its low tensile strength. Then, co-planar cracks have been incorporated in the present analysis. These cracks have been positioned in the traction zone of the cross-section (fig. 1c), which length reaches 20 mm of the concrete cover. This application assesses the probability of failure associated with depassivation of reinforcements for a service life of 60 years. Besides, four values of concrete cover depth (C) have been considered: 35 mm, 40 mm, 50 mm and 60 mm.

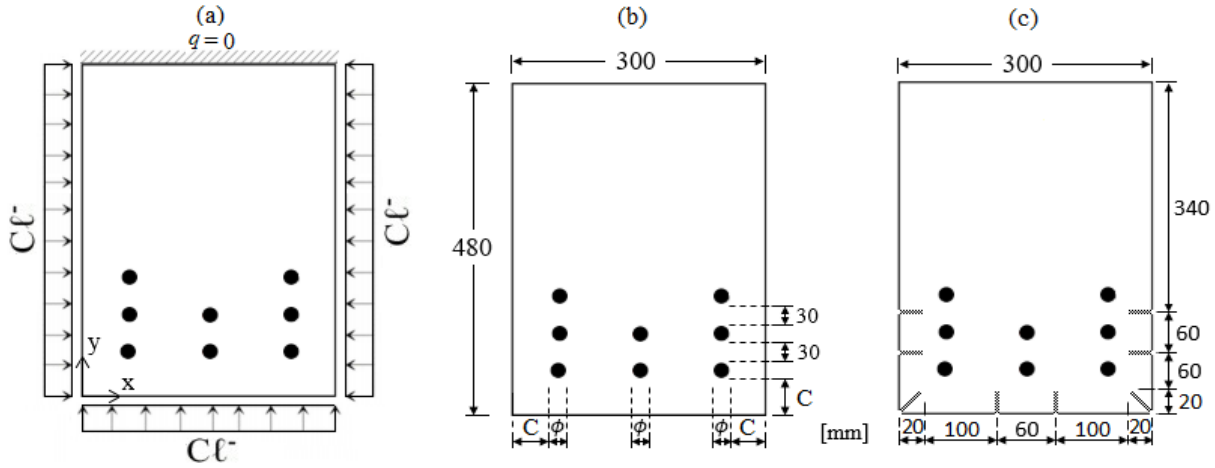

Figure 1. (a) Geometry and boundary conditions, (b) Cross-section dimension, (c) Crack positions

Three parameters are random in the present analyses: concentration of surface chloride (C_0), threshold chloride content (C_r) and the diffusion coefficient of chloride in concrete (k_c). The statistical properties attributed to C_0 account for regions distant less than 0.1 km from the coastal zone [13] and k_c is a function of the water/cement ratio (w/c), which has been assumed as 0.4. Table 1 presents such statistical information.

Table 1. Statistical parameters of random variables

Parameter	Mean	COV[1]	Distribution	Reference
C_0	2.95 Kg/m³	0.70	Lognormal	McGee [13]
C_r	0.90 Kg/m³	0.19	Uniform	Stewart & Rosowsky [3]
$k_c\,(w/c{=}0.4)$	4.5E-13 m²/s	0.75	Lognormal	Papadakis et al. [14]

[1]COV, Coefficient of Variation.

The cross-section has been discretised with isoparametric lagrangian elements of quadratic approximation. The number of elements and degrees of freedom (DOF) considered herein are upon Table 2. It is worth stressing that the cross-section with cracked cover has been divided into 10 subregions. In addition, each rebar has been represented by a circular hole of 25 mm diameter, whose discretisation is composed of 8 isoparametric elements of quadratic approximation and 17 nodes. Nil flux conditions has been assumed along the reinforcements boundaries because the coefficient of diffusion of steel is small in comparison to concrete. Therefore, the problem has homogeneous domain, which justifies the adoption of a single diffusion coefficient.

The time has been discretised in 2 years time-span and 10 integration points carried out the kernels integrations. A deterministic analysis demonstrated convergence with these settings. One assumed the mean values presented in Table 1 and a reference model constructed via ANSYS [15]. The Finite Element Method (FEM) from ANSYS utilised the triangular elements PLANE 77. The mesh details from ANSYS are upon Table 2. Figure 2 illustrates the evolution of the chloride concentration along time for the most requested point on the first layer of reinforcements. The curves illustrated in this figure demonstrate the good agreement among the responses achieved by BEM and FEM. Then, 30 time steps and 10 integration points are sufficient for the numerical BEM solution.

Table 2. Number of elements (and DOF) in the boundary mesh (BEM) and domain mesh (ANSYS)

Cover [mm]	Uncracked cross-section		Cracked cross-section	
	BEM	ANSYS	BEM	ANSYS
35	90 (384)	3,010 (12,466)	138 (660)	3,096 (12,810)
40	90 (384)	3,030 (12,546)	138 (660)	3,052 (12,634)
50	90 (384)	3,024 (12,522)	138 (660)	3,062 (12,674)
60	90 (384)	3,024 (12,522)	138 (660)	3,074 (12,722)

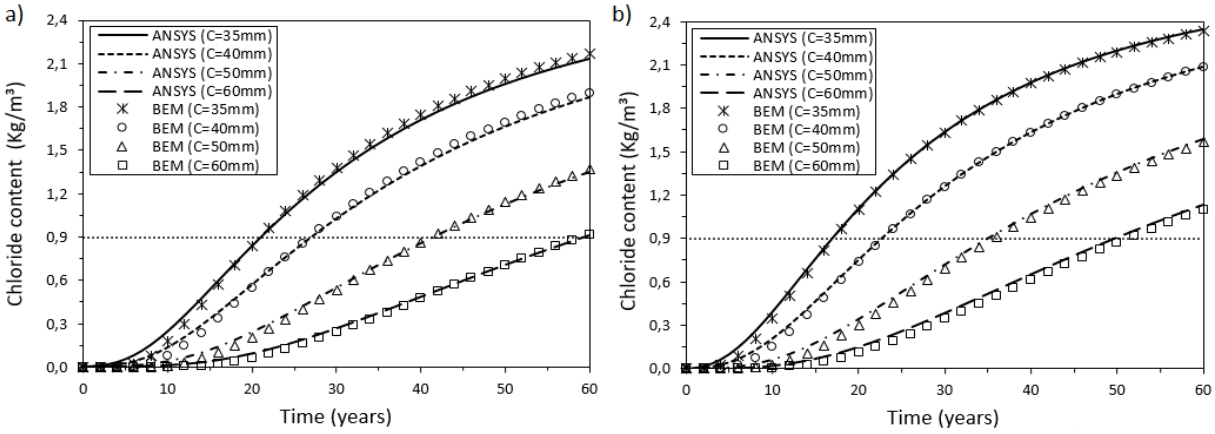

Figure 2. Chloride content as a function of time in a) uncracked and b) cracked cross-section

In the MCS, 10,000 samples were adopted, which lead to convergence in previous analyses. Figure 3 illustrates the probabilities of depassivation evolution as a function of time, which accounts for Eq. (18) at different scenarios.

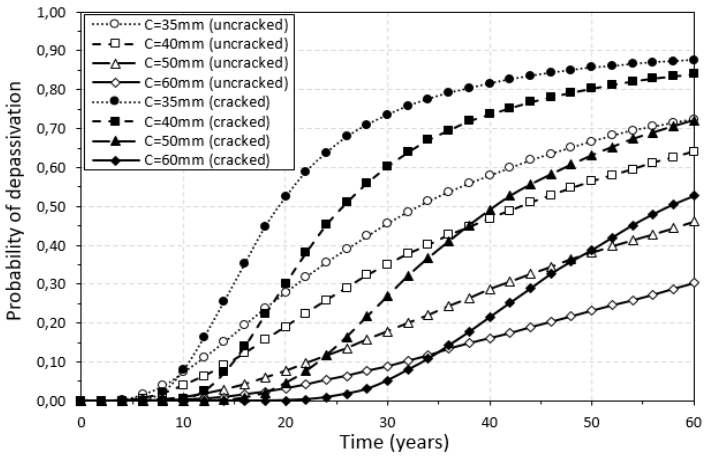

Figure 3. Probability of depassivation with cracked and uncracked cross-section

Figure 3 illustrates that the concrete cover depth has a huge influence on the probability of depassivation. At 50 years, time usually assumed as the average service life of reinforced concrete structures, such probability resulted 66.73%, 56.45%, 37.17% and 23.17%, respectively, for the uncracked covers of 35 mm, 40 mm, 50 mm and 60 mm. Besides, the probability of depassivation is more critical in the cracked cover case and reaches 85.72% (C = 35 mm), 80.33% (C = 40 mm), 63.14% (C = 50 mm) and 38.75% (C = 60 mm), for the same period of time.

It is worth mentioning that the Eurocode EN 1990 [16] recommends a target reliability index of β =1.5 ($Pf \cong$ 7%) for a reference period of 50 years in the service limit state (irreversible) and moderate reliability class; while the fib Model Code [17] recommends a minimum reliability index β = 1.3 ($Pf \cong$ 10%) for depassivation triggered by chlorides from seawater or deicing salt (service limit state). One observes that the recommended values have not been obeyed in the simulations performed herein. Nevertheless, these codes do not provide clear information

about how service life have been accounted in the design, especially for chloride ingress case. A criticism of the fib model is that the calculated reliability has no meaning in relation to the corrosion distribution, requiring a review of the model [18]. According to Diamantidis & Holický [19], the reliability indexes β recommended by EN 1990 [16] do not have explicit link to the design working life. In addition, some studies suggest that depassivation does not fully fit the classic definition of service limit state, since loss of structural function does not occur with the depassivation of reinforcements. Thus, the comparison with values recommended by codes and design standards may not be adequate. Other limitations, associated with the mechanical model (such as rebar representation, constant diffusion coefficient and surface chloride concentration) or even the existence of insufficient statistical data, can contribute to epistemic uncertainties and incompatible results with the real world.

6 Conclusions

The Transient BEM approach demonstrated robustness and efficiency in the modelling of chloride diffusion into concrete pores. Besides, BEM enabled deterministic and probabilistic analyses, which lead to consistent responses. As expected, greater depths of concrete cover delayed the corrosion initiation. Nevertheless, the presence of cracks in the cover increased drastically the probability of depassivation for the analysis time. These results reinforce the importance of periodic prevention and maintenance measures for the durability of reinforced concrete structures.

Acknowledgements. The authors are grateful for the financial support provided by the Coordenação de Aperfeiçoamento de Pessoal de Nível Superior (CAPES).

Authorship statement. The authors hereby confirm that they are the sole liable persons responsible for the authorship of this work, and that all material that has been herein included as part of the present paper is either the property (and authorship) of the authors, or has the permission of the owners to be included here.

References

[1] C. Andrade; J. González. Quantitative measurements of corrosion rate of reinforcing steels embedded in concrete using polarization resistance measurements. *Materials and Corrosion*, Wiley Online Library, v. 29, n. 8, p. 515–519, 1978.
[2] O. Cascudo. Controle da corrosão de armaduras de concreto, 1ª Ed., Editora PINI Ltda., São Paulo, 1997.
[3] M. G. Stewart and D. V. Rosowsky. Time-dependent reliability of deteriorating reinforced concrete bridge decks. *Structural safety*, Elsevier, v. 20, n. 1, p. 91–109, 1998.
[4] K. Stanish; M. Thomas. The use of bulk diffusion tests to establish time-dependent concrete chloride diffusion coefficients. *Cement and Concrete Research*, Elsevier, v. 33, n. 1, p. 55–62, 2003.
[5] J. Ožbolt et al. Modelling the effect of damage on transport processes in concrete. *Construction and Building Materials*, Elsevier, v. 24, n. 9, p. 1638–1648, 2010.
[6] F. Shaikh. Effect of Cracking on Corrosion of Steel in Concrete. *International Journal of Concrete Structures and Materials*, v.12, 1-12, 2018.
[7] R. Zhang et al. Numerical investigation of chloride diffusivity in cracked concrete. *Magazine of Concrete Research*, Thomas Telford Ltd, v. 69, n. 16, p. 850–864, 2017.
[8] L. C. Wrobel. The Boundary Element Method. Applications in Thermo-Fluids and Acoustics. Wiley. v. 1, 1952.
[9] P. K. Banerjee. The boundary element methods in engineering. London: McGraw-Hill, 1994. 496 p.
[10] F. Rizzo and D. Shippy. A formulation and solution procedure for the general non-homogeneous elastic inclusion problem. *International Journal of Solids and Structures*, Elsevier, v. 4, n. 12, p. 1161–1179, 1968.
[11] M. H. Aliabadi. The boundary element method: applications in solids and structures. John Wiley & Sons, v. 2, 2002.
[12] N. Metropolis and S. Ulam. The Monte Carlo method. *Journal of the American statistical association*, Taylor & Francis, v. 44, n. 247, p. 335–341, 1949.
[13] R. McGee. Modelling of durability performance of Tasmanian bridges. In: Melchers RE, Stewart MG, editors. *Applications of statistics and probability in civil engineering*. Rotterdam: Balkema; p. 297–306, 1999.
[14] V. G. Papadakis at al. Mathematical modelling of chloride effect on concrete durability and protection measures. C*oncrete repair, rehabilitation and protection*. London, E&FN Spon, p. 165-174, 1996.
[15] ANSYS. Mechanical APDL Product Launcher R1. Student version, 2020.
[16] European Committee for Standardization. EN 1990: Eurocode - Basis of Structural Design. 2002.
[17] Fib Bulletin 34. Model code for service life design. International Federation for Structural Concrete, 2006.
[18] F. Papworth; S. Matthews. fib Model Code 2020 – Durability Design and Through Life Management of New and Existing Structures. *Sixth International Conference on Durability of Concrete Structures*. United Kingdom, 2018.
[19] D. Diamantidis and M. Holický. Reliability differentiation in the Eurocodes. *Advances and Trends in Structural Engineering, Mechanics and Computation*. CRC Press, p. 264, 2010.